Quaternary structure and biochemical properties of mycobacterial RNase E/G

Mirijam-Elisabeth Zeller, Agnes Csanadi, Andras Miczak, Thierry Rose, Thierry Bizebard, Vladimir Kaberdin

Biochemical Journal Immediate Publication. Published on 4 Jan 2007 as manuscript BJ20061530

Quaternary structure and biochemical properties of mycobacterial RNase E/G

Mirijam-Elisabeth Zeller*, Agnes Csanadi*,†, Andras Miczak†, Thierry Rose‡, Thierry Bizebard§ and Vladimir R. Kaberdin*[1]

*Max F. Perutz Laboratories, Department of Microbiology and Immunobiology, University Departments at the Vienna Biocenter, Dr. Bohrgasse 9/4, A-1030 Vienna, Austria

†Department of Medical Microbiology and Immunobiology, University of Szeged, Szeged, Hungary

‡Unité d'Immunogénétique Cellulaire, Institut Pasteur, 28 rue du Dr. Roux, 75724 Paris Cedex 15, France

§Institut de Biologie Physico-chimique, UPR CNRS 9073, 13 rue Pierre et Marie Curie, 75005 Paris, France

[1]Correspondence and materials requests:

E-mail: vladimir.kaberdin@univie.ac.at

Fax: ++43-1-4277-9546

Tel.: ++43-1-4277-54643

Biochemical Journal Immediate Publication. Published on 4 Jan 2007 as manuscript BJ20061530

SUMMARY

The RNase E/G family of endoribonucleases plays the central role in numerous posttranscriptional mechanisms in *E. coli* and, presumably, in other bacteria including human pathogens. To learn more about specific properties of RNase E/G homologues from pathogenic Gram-positive bacteria, a polypeptide comprising the catalytic domain of *M. tuberculosis* RNase E/G (MycRne) was purified and characterized *in vitro*. Here, we show that affinity-purified MycRne has a propensity to form di- and tetramers in solution and possesses an endoribonucleolytic activity, which is dependent on the 5′-phosphorylation status of RNA. Our data also indicate that the cleavage specificities of the *M. tuberculosis* RNase E/G homologue and its *E. coli* counterpart are only moderately overlapping and reveal a number of sequence determinants within MycRne cleavage sites that differentially affect the efficiency of cleavage. Finally, we demonstrate that, similar to *E. coli* RNase E, MycRne is able to cleave in an intercistronic region of the putative 9S precursor of 5S rRNA, thus suggesting a common function for RNase E/G homologues in rRNA processing.

Key words: *M. tuberculosis*, ribonuclease, 5′-end-dependence, RNA processing.

Running title: Characterization of mycobacterial RNase E/G

INTRODUCTION

The RNase E/G family of endoribonucleases is known for its essential role in RNA processing and decay in bacteria [1-4]. Our current knowledge about these enzymes mainly originates from studies of *E. coli* RNase G and RNase E, site-specific ribonucleases that preferentially cleave in A/U-rich single-stranded regions of structured RNAs.

E. coli RNase E is encoded by the *rne* gene and is indispensable for cell viability [5, 6]. Structural data obtained for an N-terminal polypeptide representing the evolutionarily conserved catalytic domain of this protein (Fig. 1) have revealed the presence of discrete folds with putative functions in RNA recognition and cleavage [7]. Moreover, these data and others [8,9] indicate that the catalytic domain exists as a homotetramer, which has two nonequivalent subunit interfaces organizing the active site of the enzyme. In contrast to the N-terminal catalytic domain, the C-terminal part of *E. coli* RNase E shows very little or no similarity to the equivalent regions of other RNase E homologues [10]. This part of the *E. coli* enzyme contains an extra RNA-binding domain(s) [11,12] and multiple sites for interactions with the 3′ to 5′ phosphorolytic exonuclease polynucleotide phosphorylase (PNPase), the RNA helicase RhlB and the glycolytic enzyme enolase [10,13] to form the *E. coli* RNA degradosome [14].

E. coli RNase G [15,16] is encoded by the *rng* gene and was initially termed CafA due to its effects on the formation of cytoplasmic axial filaments observed upon RNase G overproduction *in vivo* [17,18]. Further studies revealed that this protein has an endoribonucleolytic activity [19] and is involved in maturation of 16S rRNA *in vivo* [15,16]. Although RNase G functionally overlaps with RNase E and shares 35% identity and 50% similarity with the N-terminal catalytic part of RNase E [20], this endoribonuclease cannot fully compensate RNase E deficiency in rne^{ts} mutant strains [5,6].

Due to their overlapping functions and apparently common origin RNase E- and RNase G-like proteins are believed to belong to the same family of RNase E/G endoribonucleases that are predicted to exist in many bacteria including pathogenic species [21-23]. Although their biochemical properties and biological functions have not yet been investigated in detail in human pathogens, such studies can offer important insights concerning the role of these endoribonucleases during infection and disease development. This consideration prompted us to purify and characterize the RNase E/G homologue (MycRne) from the intracellular pathogen *M. tuberculosis*.

We have shown that, similar to *E. coli* RNase G [24] and the catalytic domain of *E. coli* RNase E [8, 9], MycRne is a 5′-end-dependent endoribonuclease, which can exist in di-

and tetrameric states in solution. Moreover, MycRne can cleave a putative 5S rRNA precursor *in vitro,* and the cleavage occurs very close to the 5′ end of mature 5S rRNA, thus suggesting a role for this endoribonuclease in rRNA processing *in vivo*. Although MycRne and *E. coli* RNase E share some common properties, we show here that their substrate specificities are only partly overlapping. Taken together, our data expand the current knowledge about biochemical characteristics of RNase E/G enzymes and provide a basis for further analysis of their putative functions in mycobacteria.

MATERIALS AND METHODS

Bacterial strains and growth conditions

E. coli strains were routinely grown in Luria Bertani (LB) medium supplemented with the appropriate antibiotic(s) and/or glucose at 37°C. *Mycobacterium bovis* BCG was grown in Middlebrook 7H9 broth (Difco) supplemented with 10% Middlebrook OADC enrichment (Difco) and 0.05% Tween 80 (Sigma).

Purification of Rne498

E. coli BL21(DE3) strain (Novagen) carrying a pET16b-based plasmid that encodes the first 498 amino acids of *E. coli* RNase E (Rne498, [12]) was used to overexpress 6His-tagged Rne498, and the overexpressed protein was further purified by immobilized metal affinity chromatography as described previously [12]. The eluate fractions, in which the purity of Rne498 was greater than 95%, were pooled, dialyzed against SB buffer (50 mM Tris/HCl, pH 8.0, 0.1 mM EDTA, 0.5 M NaCl, 20% (v/v) glycerol and 1 mM dithiotreitol) and stored in small aliquots at –80^{o}C.

Purification of *M. tuberculosis* RNase E/G

A 1.8 kb DNA fragment (gene MT2520) encoding the C-terminal portion of mycobacterial RNase E/G polypeptide (MycRne, residues 332-953) was amplified from genomic DNA using primers Myc3 (5′-TAACATATGGTGGTGCGCGACC-3′) and Myc2 (5′-CGGAGA TCTGGTCAGTCTAGGCGG-3′). The NdeI/BglII-digested PCR product was ligated into NdeI/BamHI-treated p6HisF-11d (*icl*) [25] downstream of the T7 RNA polymerase promoter and in frame with the preceding sequence of the N-terminal 6His-tag. The resulting construct was named pMtRne, verified by sequencing and transformed into the *E. coli* strain BL21-CodonPlus (DE3)-RIL (Stratagene).

E. coli cells containing pMtRne plasmid were grown at 37°C in LB supplemented with ampicillin (100 μg/ml), chloramphenicol (34 μg/ml) and glucose (0.75%). At an OD_{600} ~0.5, the cell culture was pre-cooled on ice for 45 min, and protein expression was induced by addition of IPTG to 1 mM and incubated for 16 h at 15°C further. Cells were harvested by centrifugation (15 min, 7000 g), frozen at -20°C, thawed and suspended in ice-cold binding buffer (0.5 M NaCl, 20 mM sodium phosphate, pH 7.4) supplemented with pepstatin (1 μg/ml) and protease inhibitor cocktail (1 tablet per 3 g of wet cells) (Roche). The cells were disrupted by sonication in a Cell Disruptor W375 (Heat Systems Ultrasonics Inc.), the cell lysate was further cleared by centrifugation (15 min, 16000 g, 4°C) and the supernatant was applied to a HisTrap HP (Amersham Biosciences) column to purify 6His-tagged MycRne according to the vendor's instructions. Column fractions containing MycRne were combined, supplemented with EDTA and DTT to final concentrations of 0.1 mM and 1 mM respectively, dialyzed extensively against EB buffer (50 mM NaCl, 20 mM HEPES, pH 7.5, 1 mM DTT, 0.1 mM EDTA) and further stored in small aliquots at –80°C.

Gel filtration

Affinity-purified MycRne was dialyzed against low-salt buffer (75 mM NaCl, 10 mM HEPES, pH 7.5, 1 mM DTT, 0.1 mM EDTA) and concentrated to 8.25 mg/ml employing a Centricon YM-30 device (Millipore). The concentration of MycRne was calculated based on its absorbance at 280 nm and using extinction coefficients estimated from its amino acid composition by ProtParam (ExPaSy server, www.expasy.org). Prior to loading an aliquot (~150 μl) of the concentrated protein sample on a 25-ml Superose 12 HR10/30 column (Amersham Biosciences), the column was pre-equilibrated with low-salt buffer and calibrated using molecular weight markers (aldolase (158 kDa), BSA (67 kDa) and chymotrypsinogen A (25 kDa)). The column was run using the same buffer, and 0.5 ml-fractions were subsequently collected and analyzed by spectrophotometry and SDS-polyacrylamide gel electrophoresis.

Analytical ultracentrifugation

An aliquot of affinity-purified MycRne was dialyzed against 20 mM HEPES, pH 7.5, 100 mM NaCl, 1 mM DTT, 0.1 mM EDTA and further used in sedimentation equilibrium experiments, which were performed at 20°C on a Beckman Optima XL-A ultracentrifuge with an AN60-Ti rotor. The same buffer was used to dilute samples and as a blank. Long runs were performed at 6 speeds (5, 6, 7, 9.5, 12 and 45 krpm) using 150 μl samples at 3 concentrations (16 μM, 8 μM and 1.6 μM) analysed at 292, 286 and 233 nm, respectively;

whereas short runs were processed at 10 speeds (5, 6, 7, 9.5, 12, 14, 16, 18, 20 and 45 krpm) using 40 µl samples at 3 concentrations (84 µM, 42 µM and 16 µM) analysed at 297, 292 and 286 nm, respectively. Absorbance analysis (220 to 320 nm) revealed that the equilibrium at 5 krpm was reached after 2 and 18 hours for 40 µl and 150 µl samples, respectively. Absorbance profiles were recorded 5 times with a step of 0.001 cm for every speed and fitted simultaneously on single species or self-association models. The molar extinction coefficient at 280 nm was computed from the protein sequence as ε_{280} = 33200 $M^{-1}cm^{-1}$ [26] and extrapolated from protein spectra at other wavelengths (ε_{233} = 91721 $M^{-1}cm^{-1}$, ε_{292} = 12025 $M^{-1}cm^{-1}$, ε_{297} = 2886 $M^{-1}cm^{-1}$). Variances between experimental points and best fits were used to select the models. The MycRne specific partial volume *v-bar* = 0.713 mL/g was computed from the protein sequence.

In vitro transcription and labelling of 9S RNA

A DNA fragment including the putative *Mycobacterium bovis* BCG 9S RNA sequence was PCR amplified from genomic DNA using primers 9Sfor (5′-TGCTAACCGGCCGAAAACTTA-3′) and 9Srev (5′-AACATACAAAAACACCACCGT-3′), and cloned into the pGEM®-T Easy vector (Promega) at the T cloning site. The resulting plasmid (pMt9S) was further verified by sequencing, linearized by PstI (MBI), blunted with Klenow enzyme (MBI), purified in a 1% agarose gel and used to transcribe 9S RNA with a MEGAscript® T7 kit (Ambion). 9S RNA was further purified from a 6% polyacrylamide /urea gel, dephosphorylated with bacterial alkaline phosphatase (MBI Fermentas) and 5′-labelled using T4 polynucleotide phosphorylase (MBI Fermentas) and an excess of [γ-^{32}P] ATP (Amersham). 5′-end labelled 9S RNA was further purified from a 6% (w/v) polyacrylamide sequencing gel as described [27] and subsequently used for cleavage assays.

Primer extension

Total RNA from *Mycobacterium bovis* BCG was extracted using the hot phenol method [28]. The 5'-[^{32}P]-labelled 5S rRNA-specific oligonucleotide 5SPEM (5′-CAG TATCATCGGCGCTGGC) and total RNA (150 ng) were co-precipitated with ethanol, the pellet was air dried and suspended in 5 µl of annealing buffer (75 mM KCl, 67 mM Tris/HCl, pH 8.3), heated to 70°C, quenched on ice, mixed with 5 µl of RT buffet (75 mM Tris/HCl, pH 8.3, 20 mM $MgCl_2$, 4 mM DTT, 0.8 mM each dNTP) containing 4 units of AMV reverse transcriptase (Promega) and incubated for 30 min at 42°C. The reaction was stopped by adding 10 µl of sequencing dye. The sample was denatured at 95°C for 3 min and further

analyzed on an 8% sequencing gel along with a concurrently run sequencing ladder. The latter was prepared using *Pst*I-digested pMt9S, the same 5'-[^{32}P]-labelled primer and a Reader^{TM} DNA sequencing kit (MBI Fermentas).

Synthetic oligonucleotide substrates

Ribooligonucleotides 5′-ACAGUAUUUG (BR10), 5′-ACAGAAUUUG (9SA) 5′-GAAGGAUUUAA (OmpC), 5′-AAAAAAAAAAAAAAAAAAAAAAAAA (A27), 5′-UUUUUUUUUUUUUUUUUUUUUUUUU (U27), 5′-UUUUUUUUUUUUGUUUU-UUUUUUUUU (U27G), 5′-UUUUUUUUUUUUUAUUUUUUUUUUUU (U27A), 5′-UUUUUUUUUUUUUCUUUUUUUUUUUU (U27C) as well as oligonucleotides 5′-pGGGACAGUAUUUG (pBR13-Fluor) and 5′-HOGGGACAGUAUUUG (HO-BR13-Fluor) with a fluorescein tag at their 3′ ends were purchased from VBC Genomics (Vienna), whereas UUUUUUUUUUUUXUUUUUUUUUUUU (U27Ab) containing abasic residue (X) was purchased from Dharmacon (USA).

RNase E/G cleavage of oligonucleotide substrates and 9S RNA

RNase E/G cleavage reactions were performed as described previously [27] using Rne498 (or MycRne) and 5′-labelled substrates. 1 nt ladders were prepared either by partial alkaline hydrolysis of each 5′-end labelled substrate in 1mM EDTA, 50 mM sodium carbonate (pH 9.2) at 85^{o}C for 20 min or by partial digestion of 5′-end labelled oligonucleotides with S1 nuclease in buffer provided by the vendor (MBI). RNase T_1 digests of 9S RNA were prepared by incubation of 5′-end labelled 9S RNA in 10 mM Tris/HCl, pH 8.0; 100 mM sodium chloride, and 5 mM magnesium chloride with RNase T_1 (MBI) at 37^{o}C.

RESULTS

Cloning and purification of *M. tuberculosis* RNase E/G

To learn more about organization and biochemical properties of RNase E/G from Gram-positive bacteria, the *M. tuberculosis* RNase E/G homologue was overproduced in *Escherichia coli* and purified by affinity chromatography (see Materials and Methods). Since the full-length *M. tuberculosis* RNase E/G is difficult to purify in large amounts due to its tendency to form insoluble aggregates upon overexpression (unpublished observation), we cloned its truncated form of 621 amino acids, referred to as MycRne. The amino acid sequence of MycRne includes the entire catalytic domain and the adjacent C-terminal region of this protein (Fig. 1A). The corresponding genomic fragment was amplified by PCR, ligated

into an expression vector and verified by sequencing. The recombinant MycRne carrying a 6His-tag was overexpressed in *E. coli* strain BL21-CodonPlus(DE3)-RIL and purified under native conditions. As seen in Fig. 1B, the 71 kDa MycRne protein exhibited an aberrant mobility, migrating as a 110 kDa polypeptide. Slower running of RNase E/G homologues in SDS polyacrylamide gels has been reported previously and appears to be caused by their unusual amino acid composition [29]. Mass spectrometry analysis did not reveal any contamination of the MycRne preparation by *E. coli* RNase E/G polypeptides or other host ribonucleases (data not shown).

Quaternary structure of *M. tuberculosis* RNase E/G

The putative catalytic domain of MycRne contains the highly conserved Zn-link motif known to be implicated in di- and tetramerization of *E. coli* RNase E/G [8,9]. To assess whether the ability of RNase E/G homologues to form di- and tetrameric forms is evolutionarily conserved, we analyzed the oligomerization state of affininy-purified MycRne. According to the calibration profile obtained with aldolase, BSA and chymotrypsinogen A, MycRne was eluted as a complex with a hydrodynamic radius corresponding to a spherical protein with an apparent molecular mass of approximately 325 kDa (Fig. 2A), suggesting that, similar to *E. coli* homologues, MycRne may exist in a tetrameric form.

In order to confirm the oligomerization state of MycRne by an independent method, we performed analytical ultracentrifugation (Fig. 2B). To analyze the self-association state of MycRne, sedimentation equilibrium experiments were performed at different concentrations (1.6 μM, 8 μM, 16 μM, 42 μM and 84 μM) and several speeds. The absorbance scans (fitted simultaneously on single species or self-association models) indicated an apparent molecular mass of 71,100 Da for the monomer. The records at 16 μM and 42 μM fitted best on a monomer-dimer equilibrium (1502 points/concentration, variance 0.000163) with a $K_D \approx 1.8$ μM, while the profiles at 84 μM could best be modelled as dimer-tetramer equilibrium (862 points, variance 0.000277) with a $K_D \approx 95$ μM. According to these data, the molecular species of MycRne appear mainly as monomers below concentrations of ca. 1 μM, predominantly as dimers up to ca. 100 μM and as tetramers in more concentrated solutions.

Cleavage of oligonucleotide substrates

To test whether MycRne has an endoribonucleolytic activity and to compare its specificity with that of *E. coli* RNase E, we performed cleavage assays using affinity-purified MycRne and Rne498 (*E. coli* RNase E; residues 1-498), a C-terminally truncated form of *E. coli*

RNase E representing its catalytic domain [12]. The assays were carried out with synthetic ribooligonucleotides BR10, 9SA and OmpC, all of which are well-characterized *E. coli* RNase E substrates [27, 30, 31]. As seen in Fig. 3, MycRne could cut all three oligonucleotides yielding cleavage patterns that were largely indistinguishable from the analogous patterns generated by its *E. coli* counterpart. A minor difference was only observed in the cleavage pattern of OmpC. Although Rne498 cleaved this oligonucleotide at positions 5 and 6 with equal efficiencies, MycRne showed some preference for cleavage at position 5. We also found that, similar to its RNase E/G homologues from *A. aeolicus* and *E. coli,* MycRne requires magnesium ions for its activity (Fig. 3E).

5′-end dependence of *M. tuberculosis* RNase E/G cleavages

RNase E/G homologues from Gram-negative bacteria are known to preferentially cleave 5′-monophosphorylated substrates when compared to non-phosphorylated [19,32,33] or 5′-triphosphorylated ones [34]. Employing 5′-monophosphorylated and non-phosphorylated BR13 (5′-GGGACAGUAUUUG-3′) tagged with a fluorescein group at their 3′ ends, we demonstrated that, similar to its counterparts, MycRng cleaves 5′-monophosphorylated substrates faster than the non-phosphorylated ones (Fig. 4A and B). Thus, our data suggest that the so-called 5′-end dependence is apparently a common feature of RNase E/G homologues from both Gram-negative and Gram-positive bacteria.

Probing the substrate specificity of *M. tuberculosis* RNase E/G

In order to identify specific sequence determinants of MycRne cleavage sites we used essentially the same oligonucleotide-based approach that was previously employed to characterize its *E. coli* counterpart [35]. By comparing the cleavage patterns of poly(A) and poly(U) oligonucleotides and their mutant variants carrying single-base substitutions of adenosine (or uridine) by G, C, U or A, respectively, this method allows determining the effect of each nucleotide at multiple positions to the point of cleavage [35].

Unlike *E. coli* RNase E [36, 37], MycRne cleaved A27 inefficiently. As seen in Fig. 5A, despite 5 fold excess of MycRne (when compared to the cleavage conditions of U27), A27 cleavage products can be readily detected only on overexposed X-ray films (Fig. 5A). In the following assays, we therefore decided to use only U27 (control) and its derivatives, U27A, U27G, U27C and U27ab oligonucleotides, that had a single base substitution of U at position 14 by either A, G, C or abasic residue, respectively.

Similar to cleavage of U27 (Fig. 5B), incubation of U27G with MycRne and Rne498 resulted in nearly identical patterns (Fig. 6A). The major cleavages of U27G at positions U8, U9, U10 and U15 were observed for both enzymes, whereas Rne498 (but not MycRne) could additionally cleave this substrate at position U18. In the case of *E. coli* RNase E, it has been previously reported that a G nucleotide, which is 5´ and in close vicinity to the scissile bond, is an important determinant of cleavage [31,33,35]. Likewise, we found that *M. tuberculosis* RNase E/G cleavage is more efficient if there is a G nucleotide located 2 nucleotides upstream of the scissile bond (Fig. 6A). These data are fully consistent with the cleavage patterns of BR10, 9SA and OmpC oligonucleotides showing that MycRne cleavage frequently occurs 2 nucleotides downstream of a G nucleotide (Fig. 3).

In contrast to nearly identical cleavage patterns that were generated by MycRne and Rne498 using U27G (Fig. 6A), the cleavage patterns of U27A, U27C and U27ab showed relatively low resemblance (Fig. 6B, C and D, respectively). Although Rne498 can cut at multiple positions within U27A (Fig. 6B), MycRne cleavage of the same substrate was not observed at many of these locations, especially downstream and upstream of U16. Similarly, the presence of a cytosine at position 14 in U27C (Fig. 6C) strongly inhibits MycRne (and to a lesser degree Rne498) cleavage at nearly all locations suggesting the overall inhibiting effect of this nucleotide. Finally, we found that substitution of the U at position 14 by an abasic residue in U27ab (Fig. 6D) decreased the efficiency of MycRne cleavage at multiple locations. This finding strongly suggests that the presence of uridines at many locations close to the scissile bond promotes MycRne cleavage.

Based on the above experimental data, we determined and summarized the effects of each nucleotide within MycRne cleavage sites (Fig. 6E). Interestingly, according to these data, the C at position +2 in 9SA should confer higher resistance of this oligonucleotide (in comparison to BR10 lacking a cytosine at the equivalent position) to MycRne. In contrast, we did not observe any significant differences in the efficiency of cleavage (Fig. 3, unpublished data). This may imply that the expected inhibiting effect of the cytosine was efficiently counteracted by other nucleotides, for example, by the A and G nucleotides at positions -3 and -2, respectively. In other words, strong enhancing effects of nucleotides at certain positions of different cleavage sites can potentially neutralize / override negative effects of other sequence determinants, resulting in approximately equal efficiency of cleavage.

Like in the case of *E. coli* RNase E [35,37], the efficiency of MycRne cleavage of U27 and its mutant variants decreases with the number of the remaining nucleotides that are

5′ to the scissile bond (the "end-proximity effect"), thereby leading to accumulation of short oligomers that are further resistant to the nucleolytic activity of this enzyme.

9S RNA processing by *M. tuberculosis* RNase E/G

While playing an essential role in maturation of stable RNA in *E. coli*, RNase E is known to process the 9S RNA precursor of the 5S rRNA [38]. To find out whether MycRne might act likewise in the processing of rRNA in *M. tuberculosis*, we examined the cleavage pattern obtained after incubation of *in vitro* transcribed *M. tuberculosis* 9S RNA with Rne498 and MycRne. Although both enzymes could cleave this RNA, the cleavages occurred at different locations (Fig. 7A, on the left). This finding is consistent with our data (Fig. 6) suggesting some differences in the substrate specificities of *E. coli* and *M. tuberculosis* RNase E/G homologues. Further analysis (Fig. 7B, on the right) revealed that MycRng cleaved 9S RNA at the position, which nearly coincides with the position of the 5′ end of mature 5S rRNA *in vivo,* which was mapped by primer extension of total RNA (Fig. 7B and C).

DISCUSSION

Mycobacteria are Gram-positive bacteria known to enter a state of metabolic dormancy when they encounter anoxic or nutritionally deprived environments [39]. This mechanism allows pathogenic species such as *M. tuberculosis* to survive within their host-cells and involves numerous changes in gene expression to convey the required physiological adjustments. Adaptive processes in the RNA metabolism of latent mycobacteria differentially affect the steady-state levels of numerous transcripts [40], ribosome biosynthesis [41] as well as RNase E/G level [42], suggesting an important regulatory role of this enzyme during the disease development. To learn more about the function and biochemical properties of the RNase E/G homologue from *M. tuberculosis* (MycRne), we cloned, purified and characterized a polypeptide including the centrally located catalytic domain as well as the flanking C-terminal part of this protein (Fig. 1).

We found that, similar to its homologues, *E. coli* RNase E (residues 1-530; [7-9]) and RNase G [24] polypeptides, purified MycRne can exist in solution in di- or tetrameric forms. Previous work has shown that a pair of cysteine residues in the conserved CPxCxGxG motif, which coordinates a zinc ion (so-called Zn-link motif), is critical for assembly of the *E. coli* RNase E homotetramers [7]. Given that the Zn-link motif exists in MycRne and other members of the RNase E/G family, our results suggest that the protein-protein interfaces,

which are involved in intermolecular association of MycRne (this study) and its *E. coli* counterparts [7-9, 24] apparently resemble each other and that the association as dimer-of-dimers may be a common feature of RNase E/G homologues. Interestingly, although the tetrameric form of the catalytic domain of *E. coli* RNase E (amino acid residues 1-530) is more active *in vitro* than the monomeric one [9], a truncated *E. coli* RNase E polypeptide (amino acid residues 1-395), which retains an endoribonucleolytic activity (but has no potential to self-associate), can functionally substitute the full-length *E. coli* RNase E *in vivo* [43]. Although this finding suggests that bacterial cells can survive with RNase E functioning as a monomer, a tetrameric quaternary structure of this enzyme may be still important to confer efficient cleavage of RNA in fast-growing cells.

By employing oligonucleotide substrates, we have also shown that MycRne has an endoribonucleolytic activity, which is dependent on the 5′ phosphorylation status of its substrates, thereby suggesting that MycRne is a 5′-end-dependent endoribonuclease. This property of MycRne (this study) and other RNase E/G homologues [19,32,34,44,45] implies that these enzymes more efficiently cleave already damaged or partly degraded forms of cellular RNAs (i.e. RNA species that usually carry 5′-monophosphate groups) rather than primary transcripts, which are naturally triphosphorylated.

The enzyme can cleave short oligonucleotides with the specificity, which is similar to that observed previously for *E. coli* RNase E (Fig. 3). However, despite their seemingly indistinguishable sequence specificities (Fig. 3), further analysis using homooligomeric substrate U27 and its monosubstituted derivatives U27A, U27C, U27G and U27ab (Fig. 6) revealed a number of important differences in the optimal location of G, C, U and A nucleotides within *E. coli* RNase E and MycRne cleavage sites. Both endoribonucleases cleave more efficiently in the presence of a G nucleotide upstream of and in close proximity to the point of cleavage. However, unlike *E. coli* RNase E sites that are usually rich in A/U nucleotides [35, 46, 47], MycRne apparently prefers to cleave sequences enriched mainly in U (but not A) nucleotides. Likewise, the C in U27C differentially affects cleavages by *E. coli* and *M. tuberculosis* RNase E/G homologues. When placed in certain locations close to the scissile bond, the cytosine not only inhibits but also enhances the efficiency of *E. coli* RNase E cleavages ([35], Fig. 6C), whereas, in the case of *M. tuberculosis* RNase E/G, it only inhibits cleavage at nearly every position. This study and others [19,32] demonstrate that the substrate specificity of RNase E/G endoribonucleases can significantly vary and cannot be easily inferred from previous data that were obtained for a particular RNase E/G homologue.

Our recent work demonstrate that the knowledge of specific sequence determinants within RNase E/G cleavage sites can be instructive to suggest mutations that increase/decrease the efficiency of cleavage within the site of interest [35] and to infer differences in the substrate specificities of various RNase E/G homologues (this study). However, this information may not be sufficient *per se* to predict potential RNase E cleavage sites within a regular transcript. Additional factors such as RNA structure or interactions with RNA-binding proteins should be also taken into consideration.

Given that RNase E and RNase G are involved in maturation of ribosomal and transfer RNAs in *E. coli* [48,49], we anticipated that this function of RNase E/G-like proteins might be also conserved in mycobacteria. Indeed, we found that MycRne was able to cleave mycobacterial 9S RNA (Fig. 7A), a putative precursor of its cognate 5S rRNA, and the cleavage occurred in close vicinity to the mature 5′-end of 5S rRNA (Fig. 7B and C), thereby suggesting a role for this enzyme in rRNA processing. Although the internucleotide bonds at the 5′ end of 5S rRNA, that are generated by MycRne *in vitro* (Fig. 7A) and during rRNA processing *in vivo* (Fig. 7B) were not exactly the same, this minor (1-2 nucleotide) difference could be well explained by the action of ancilliary factors or associated ribosomal proteins that can affect MycRne cleavage *in vivo* and, therefore, slightly influence the selection of the scissile bond(s). Further efforts will be necessary to get a better understanding of diverse roles of MycRne in RNA processing and to reveal and characterize the MycRne-mediated, post-transcriptional mechanisms that are involved in adaptive stress responses and the associated alterations in RNA metabolism in mycobacteria.

ACKNOWLEDGEMENTS

We thank Dr. Denise Barlow for critically reading the manuscript. This work was supported by grant no. F1707 from the Austrian Science Foundation (V.R.K.), by CNRS (T.R. and T.B.), and by OTKA 034820 from the Hungarian Scientific Research Fund (A.M.). A.Cs. was a recipient of the FEMS and Hungarian State Eötvös fellowships.

REFERENCES

1 Cohen, S.N., and McDowall, K.J. (1997). RNase E: Still a wonderfully mysterious enzyme. Mol. Microbiol. **23**, 1099-1106.

2 Coburn, G.A., and Mackie, G.A. (1999). Degradation of mRNA in *Escherichia coli*: An old problem with some new twists. Prog. Nucleic Acids Res. Mol. Biol. **62**, 55-108.

3 Régnier, P., and Arraiano, C.M. (2000). Degradation of mRNA in bacteria: emergence of ubiquitous features. Bioessays **22**, 235-244.

4 Kushner, S.R. (2002). mRNA decay in *Escherichia coli* comes of age. J. Bacteriol. **184**, 4658-4665.

5 Deana, A., and Belasco, J.G. (2004). The function of RNase G in Escherichia coli is constrained by its amino and carboxyl termini. Mol. Microbiol. **51**, 1205-1217.

6 Ow, M.C., Perwez, T., and Kushner, S.R. (2003). RNase G of *Escherichia coli* exhibits only limited functional overlap with its essential homologue, RNase E. Mol. Microbiol. **49**, 607-622.

7 Callaghan, A.J., Marcaida, M.J., Stead, J.A., McDowall, K.J., Scott, W.G., and Luisi, B.F. (2005). Structure of *Escherichia coli* RNase E catalytic domain and implications for RNA turnover. Nature (London) **437**, 1187-1191.

8 Callaghan, A.J., Grossmann, J.G., Redko, Y.U., Ilag, L.L., Moncrieffe, M.C., Symmons, M.F., Robinson, C.V., McDowall, K.J., and Luisi, B.F. (2003). Quaternary structure and catalytic activity of the *Escherichia coli* ribonuclease E amino-terminal catalytic domain. Biochemistry **42**, 13848-13855.

9 Callaghan, A.J., Redko, Y., Murphy, L.M., Grossmann, J.G., Yates, D., Garman, E., Ilag, L.L., Robinson, C.V., Symmons, M.F., McDowall, K.J., and Luisi, B.F. (2005). "Zn-link": a metal-sharing interface that organizes the quaternary structure and catalytic site of the endoribonuclease, RNase E. Biochemistry *44*, 4667-4675.

10 Kaberdin, V.R., Miczak, A., Jakobsen, J.S., Lin-Chao, S., McDowall, K.J., and von Gabain, A. (1998). The endoribonucleolytic N-terminal half of *Escherichia coli* RNase E is evolutionarily conserved in *Synechocystis sp.* and other bacteria but not the C-terminal half, which is sufficient for degradosome assembly. Proc. Natl. Acad. Sci. USA **95**, 11637-11642.

11 Leroy, A., Vanzo, N.F., Sousa, S., Dreyfus, M., and Carpousis, A.J. (2002). Function in *Escherichia coli* of the non-catalytic part of RNase E: role in the degradation of ribosome-free mRNA. Mol. Microbiol. **45**, 1231-1243.

12 McDowall, K.J., and Cohen, S.N. (1996). The N-terminal domain of the rne gene product has RNase E activity and is non-overlapping with the arginine-rich RNA-binding site. J. Mol. Biol. **255**, 349-355.

13 Vanzo, N.F., Li, Y.S., Py, B., Blum, E., Higgins, C.F., Raynal, L.C., Krisch, H.M., and Carpousis, A.J. (1998). Ribonuclease E organizes the protein interactions in the *Escherichia coli* RNA degradosome. Genes Dev. **12**, 2770-2781.

14 Marcaida, M.J., Depristo, M.A., Chandran, V., Carpousis, A.J., and Luisi, B.F. (2006). The RNA degradosome: life in the fast lane of adaptive molecular evolution. Trends Biochem. Sci. **31**, 359-365.

15 Wachi, M., Umitsuki, G., Shimizu, M., Takada, A., and Nagai, K. (1999). *Escherichia coli cafA* gene encodes a novel RNase, designated as RNase G, involved in processing of the 5' end of 16S rRNA. Biochem. Biophys Res. Commun. **259**, 483-488.

16 Li, Z., Pandit, S., and Deutscher, M.P. (1999). RNase G (CafA protein) and RNase E are both required for the 5′ maturation of 16S ribosomal RNA. EMBO J. **18**, 2878-2885.

17 Okada, Y., Wachi, M., Hirata, A., Suzuki, K., Nagai, K., and Matsuhashi, M. (1994). Cytoplasmic axial filaments in *Escherichia coli* cells: possible function in the mechanism of chromosome segregation and cell division. J. Bacteriol. **176**, 917-922.

18 Okada, Y., Shibata, T., and Matsuhashi, M. (1993). Possible function of the cytoplasmic axial filaments in chromosomal segregation and cellular division of *Escherichia coli*. Sci. Prog. **77**, 253-264.

19 Tock, M.R., Walsh, A.P., Carroll, G., and McDowall, K.J. (2000). The CafA protein required for the 5'-maturation of 16 S rRNA is a 5'- end-dependent ribonuclease that has context-dependent broad sequence specificity. J. Biol. Chem. *275*, 8726-8732.

20 McDowall, K.J., Hernandez, R.G., Lin-Chao, S., and Cohen, S.N. (1993). The *ams-1* and *rne-3071* temperature-sensitive mutations in the *ams* gene are in close proximity to each other and cause substitutions within a domain that resembles a product of the *Escherichia coli mre* locus. J. Bacteriol. *175*, 4245-4249.

21 Carpousis, A.J. (2002). The *Escherichia coli* RNA degradosome: structure, function and relationship in other ribonucleolytic multienzyme complexes. Biochem. Soc. Trans. **30**, 150-155.

22 Condon, C., and Putzer, H. (2002). The phylogenetic distribution of bacterial ribonucleases. Nucl. Acids Res. **30**, 5339-5346.

23 Lee, K., and Cohen, S.N. (2003). A *Streptomyces coelicolor* functional orthologue of *Escherichia coli* RNase E shows shuffling of catalytic and PNPase-binding domains. Mol. Microbiol. **48**, 349-360.

24 Briant, D.J., Hankins, J.S., Cook, M.A., and Mackie, G.A. (2003). The quaternary structure of RNase G from *Escherichia coli*. Mol. Microbiol. **50**, 1381-1390.

25 Honer Zu Bentrup, K., Miczak, A., Swenson, D.L., Russell, D.G. (1999). Characterization of activity and expression of isocitrate lyase in *Mycobacterium* avium and *Mycobacterium tuberculosis*. J. Bacteriol. **181**, 7161-7167.

26 Pace, C.N., Vajdos, F., Fee, L., Grimsley, G., and Gray, T. (1995). How to measure and predict the molar absorption coefficient of a protein. Protein Sci. **4**, 2411-2423.

27 McDowall, K.J., Kaberdin, V.R., Wu, S.W., Cohen, S.N., and Lin-Chao, S. (1995). Site-specific RNase E cleavage of oligonucleotides and inhibition by stem-loops. Nature **374**, 287-290.

28 Lin-Chao, S., and Bremer, H. (1986). Effect of the bacterial growth rate on replication control of plasmid pBR322 in *Escherichia coli*. Mol. Gen. Genet. **203**, 143-149.

29 Casaregola, S., Jacq, A., Laoudj, D., McGurk, G., Margarson, S., Tempete, M., Norris, V., and Holland, I.B. (1992). Cloning and analysis of the entire *Escherichia coli ams* gene. *ams* is identical to hmp1 and encodes a 114 kDa protein that migrates as a 180 kDa protein. J. Mol. Biol. **228**, 30-40.

30 Afonyushkin, T., Moll, I., Bläsi, U., and Kaberdin, V.R. (2003). Temperature-dependent stability and translation of *Escherichia coli ompA* mRNA. Biochem. Biophys. Res. Commun. **311**, 604-609.

31 Kaberdin, V.R., Walsh, A.P., Jakobsen, T., McDowall, K.J., and von Gabain, A. (2000). Enhanced cleavage of RNA mediated by an interaction between substrates and the arginine-rich domain of *E. coli* ribonuclease E. J. Mol. Biol. **301**, 257-264.

32 Kaberdin, V.R., and Bizebard, T. (2005). Characterization of Aquifex aeolicus RNase E/G. Biochem. Biophys. Res. Commun. **327**, 382-392.

33 Redko, Y., Tock, M.R., Adams, C.J., Kaberdin, V.R., Grasby, J.A., and McDowall, K.J. (2003). Determination of the catalytic parameters of the N-terminal half of *E. coli* ribonuclease E and the identification of critical functional groups in RNA substrates. J. Biol. Chem. **278**, 44001-44008.

34 Mackie, G.A. (1998). Ribonuclease E is a 5'-end-dependent endonuclease. Nature (London) **395**, 720-723.

35 Kaberdin, V.R. (2003). Probing the substrate specificity of *Escherichia coli* RNase E using a novel oligonucleotide-based assay. Nucl. Acids Res. **31**, 4710-4716.

36 Huang, H.J., Liao, J., and Cohen, S.N. (1998). Poly(A)- and poly(U)-specific RNA 3' tail shortening by *E. coli* ribonuclease E. Nature (London) **391**, 99-102.

37 Walsh, A.P., Tock, M.R., Mallen, M.H., Kaberdin, V.R., von Gabain, A., and McDowall, K.J. (2001). Cleavage of poly(A) tails on the 3′-end of RNA by ribonuclease E of *Escherichia coli*. Nucl. Acids Res. **29**, 1864-1871.

38 Ghora, B.K., and Apirion, D. (1978). Structural analysis and *in vitro* processing to p5 rRNA of a 9S RNA molecule isolated from an *rne* mutant of *E. coli*. Cell *15*, 1055-1066.

39 Cardona, P.J., and Ruiz-Manzano, J. (2004). On the nature of *Mycobacterium tuberculosis*-latent bacilli. Eur. Respir. J. **24**, 1044-1051.

40 Schnappinger, D., Ehrt, S., Voskuil, M.I., Liu, Y., Mangan, J.A., Monahan, I.M., Dolganov, G., Efron, B., Butcher, P.D., Nathan, C., and Schoolnik, G.K. (2003). Transcriptional adaptation of *Mycobacterium tuberculosis* within Macrophages: Insights into the phagosomal environment. J. Exp. Med. **198**, 693-704.

41 Beste, D.J., Peters, J., Hooper, T., Avignone-Rossa, C., Bushell, M.E., and McFadden, J. (2005). Compiling a molecular inventory for *Mycobacterium bovis* BCG at two growth rates: evidence for growth rate-mediated regulation of ribosome biosynthesis and lipid metabolism. J. Bacteriol. **187**, 1677-1684.

42 Archuleta, R.J., Yvonne Hoppes, P., and Primm, T.P. (2005). *Mycobacterium avium* enters a state of metabolic dormancy in response to starvation. Tuberculosis (Edinb) **85**, 147-158.

43 Caruthers, J.M., Feng, Y., McKay, D.B., and Cohen, S.N. (2006). Retention of core catalytic functions by a conserved minimal RNase E peptide that lacks the domain required for tetramer formation. J. Biol. Chem. **281**, 27046-27051.

44 Jiang, X., Diwa, A., and Belasco, J.G. (2000). Regions of RNase E important for 5'-end-dependent RNA cleavage and autoregulated synthesis. J. Bacteriol. **182**, 2468-2475.

45 Lin-Chao, S., and Cohen, S.N. (1991). The rate of processing and degradation of antisense RNAI regulates the replication of ColE1-type plasmids *in vivo*. Cell **65**, 1233-1242.

46 McDowall, K.J., Lin-Chao, S., and Cohen, S.N. (1994). A+U content rather than a particular nucleotide order determines the specificity of RNase E cleavage. J. Biol Chem. **269**, 10790-10796.

47 Lin-Chao, S., Wong, T.T., McDowall, K.J., and Cohen, S.N. (1994). Effects of nucleotide sequence on the specificity of *rne*-dependent and RNase E-mediated cleavages of RNAI encoded by the pBR322 plasmid. J. Biol. Chem. **269**, 10797-10803.

48 Misra, T.K., and Apirion, D. (1979). RNase E, an RNA processing enzyme from *Escherichia coli*. J. Biol. Chem. **254**, 11154-11159.

49 Li, Z., and Deutscher, M.P. (2002). RNase E plays an essential role in the maturation of *Escherichia coli* tRNA precursors. RNA **8**, 97-109.

FIGURE LEGENDS

Fig. 1. Purification of MycRne.

(A) Primary structures of *E. coli* and *M. tuberculosis* RNase E/G homologues. The evolutionarily conserved minimal catalytic domain [43] is shown by black boxes in the full-length of *E. coli* RNase E, RNase G and *M. tuberculosis* RNase E/G (MycRne (FL)) polypeptides as well as in the N-terminally truncated form of *M. tuberculosis* RNase E/G (MycRne) used in this study. The `protein scaffold` region (back-hatched box) of *E. coli* RNase E (residues 688-1061; [13]) is the location of the binding sites for the major components of the degradosome (enolase, RhlB RNA helicase and polynucleotide phosphorylase (PNPase)).

(B) Purification of MycRne. Affinity-purified mycobacterial MycRne as well as protein extracts prepared from BL21 (DE3) cells harbouring the MycRne-coding plasmid before (-) and after (+) addition of IPTG, respectively, were analyzed in 10% SDS gels followed by Coomassie blue staining. Indicated are the positions of *M. tuberculosis* RNase E/G (MycRne) and the size of several proteins in the molecular weight protein marker (lane M).

Fig. 2. Quaternary structure of RNase E/G.

(A) Gel filtration of MycRne. Affinity-purified MycRne (bold curve) was analyzed by size-exclusion chromatography using a 25 ml-Superose® 12 HR 10/30 column (Amersham Biosciences) connected to an FPLC system. The column was calibrated with aldolase (158 kDa), BSA (67 kDa) and chymotrypsinogen A (25 kDa) (light curve). Elution profiles were recorded online; the absorbance at 280 nm is indicated on the y-axis, whereas elution volumes are indicated on the x-axis.

(B) Sedimentation equilibrium analysis. A representative radial concentration distribution of RNase E/G at 16 µM is shown after reaching equilibrium (18h) at 12000 rpm at 20ºC. The lower panel plots the absorbance (OD) at 292 nm against the radial position (cm). The absorbance offset was set to 0.022 OD. The best fit of the data set (6 speeds, 1,502 points) was consistent at this sample concentration with a monomer-dimer equilibrium (solid lines) with a K_d = 1.8 µM. Residual values between experimental data and a self associating model of ideal species (molecular weight = 71,100 Da) are reported in the upper panel.

Fig. 3. Cleavage patterns of oligonucleotides BR10, 9SA and OmpC.

Each 5′ end labelled oligonucleotide (panel **A, B** and **C**, respectively) was incubated without enzyme (control), affinity-purified *E. coli* RNase E (Rne498) or *M. tuberculosis* RNase E/G (MycRne), and aliquots withdrawn at times indicated above each lane were analyzed on 20%

polyacrylamide / urea gels. Lanes S1, 1 nt ladder generated by partial digestion of BR10, 9SA or OmpC with S1 nuclease, respectively. The sequence of BR10, 9SA and OmpC is shown in panel **D**. The internucleotide bonds that are sensitive to MycRne cleavage are indicated by triangles. Filled triangles point towards the bonds that have higher sensitivity to the endonucleolytic activity of MycRne. **(E)** Magnesium dependence of MycRne cleavages. BR10 was incubated with MycRne in the absence (-) or presence (+) of magnesium ions and aliquots withdrawn at times indicated above each lane were analyzed on a 15% sequencing gel. Each assay was repeated at least twice and one representative gel image is shown.

Fig. 4. 5´-end dependence of MycRne cleavages.

(A) Relative efficiency of MycRne cleavage of fluorescently labelled 5´-phosphorylated and non-phosphorylated oligonucleotides (P-BR13-Fluor and HO-BR13-Fluor, respectively). Each oligonucleotide (~5 pmol) was incubated without (control) or with affinity-purified MycRne) and aliquots withdrawn at times indicated above each lane were analyzed on a 15% (w/v) sequencing-type gel. The signals corresponding to the fluorescently labeled oligonucleotides and their products of cleavage were visualized using a PhosphorImager (Typhoon 8600, Molecular Dynamics) and further quantified employing IMAGEQUANT software.

(B) Graphical representation of uncleaved RNA (%) plotted as a function of time (min) indicates that MycRne cleaves the 5´-phosphorylated substrate faster than the non-phosphorylated one. The graph represents the data from one single experiment, which was repeated twice with similar results.

Fig. 5. Comparative cleavage of A27 and U27 by MycRne.

(A) 5´ end labelled A27 (on the left) or U27 (on the right) were incubated without enzyme (control) or with 1.5-0.3 µg of native *M. tuberculosis* RNase E/G (MycRne), and aliquots withdrawn at times indicated above each lane were analyzed on 15% polyacrylamide / urea gels. The 1-nt ladders (lane S1) were generated by partial digestion of A27 and U27 with S1 nuclease, respectively. Each experiment was repeated at least twice and one representative gel image is shown.

(B) Cleavage patterns of U27 generated by of Rne498 and MycRne. 5´ end labelled U27 was incubated without enzyme (control), with *E. coli* RNase E (Rne498) or with *M. tuberculosis* RNase E/G (MycRne) and aliquots withdrawn at times indicated above each lane were analyzed on a 15% polyacrylamide/ urea gel. Lane S1, a 1 nt ladder prepared by partial digestion of U27 with S1 nuclease. The coordinates of U_1 and U_8 within U27 are indicated.

Internucleotide bonds with a moderate (open triangles) or high (filled triangles) sensitivity to MycRne cleavage are indicated in a schematic view of U27 shown at the bottom. Each experiment was repeated at least twice and one representative gel image is shown.

Fig. 6. Cleavage patterns of U27A, U27G, U27C and U27ab generated by Rne498 and MycRne.

Each 5′ end labelled substrate derived from U27 by replacement of the U at position 14 by an G (U27G), A (U27A), C (U27C) or abasic (U27ab) residue was incubated without enzyme (control), with *E. coli* RNase E (Rne498) or with *M. tuberculosis* RNase E/G (MycRne), and aliquots withdrawn at times indicated above each lane were analyzed on 15% polyacrylamide/ urea gels (panels **A, B, C** and **D**, respectively). Indicated are the positions of several nucleotides including the substituted base (A, G, C or the abasic residue (X), respectively) as well as site(s) sensitive to MycRne cleavage. Lane S1, 1 nt ladders generated by partial digestion of each oligonucleotide with S1. Similar patterns were obtained for each substrate in three independent experiments.

(E) Schematic views of the substrates. The internucleotide bonds with a moderate and high susceptibility to MycRne cleavage are pointed out by open and filled triangles, respectively.

Fig. 7. 9S RNA processing *in vitro* and *in vivo*.

(A) 5′-end labelled mycobacterial 9S RNA was incubated without enzyme (control), with *E. coli* RNase E (Rne498) or with *M. tuberculosis* RNase E/G (MycRne). Aliquots were withdrawn at times indicated above each lane and analyzed on 10% polyacrylamide / urea gels. The position of *M. tuberculosis* RNase E/G cleavage site (∗) was determined employing concomitantly run partial alkaline (L) and RNase T_1 (T1) digests of the same transcript shown on the right. The experiment was repeated three times with similar results.

(B) Primer extension analysis of total mycobacterial RNA (lane E) was performed using a 5′-[^{32}P]-labelled primer specific for 5S rRNA. The 5′-end of the *in vivo* processed 5S rRNA was determined by employing a concomitantly run sequencing ladder (lanes C, T, A and G) generated with the same primer (for details, see Materials & Methods). The experiment was repeated twice with similar results.

(C) The sequence of *M. tuberculosis* 5S rRNA (highlighted with grey shading) and its 5′ end flanking region. A long horizontal arrow shows the direction and position of the primer used for primer extension. The position of *in vitro* (see panel A) and *in vivo* (panel B) MycRne cleavage sites that were mapped close to the 5′ end of 5S rRNA are indicated by a single upward and two downward arrows, respectively.

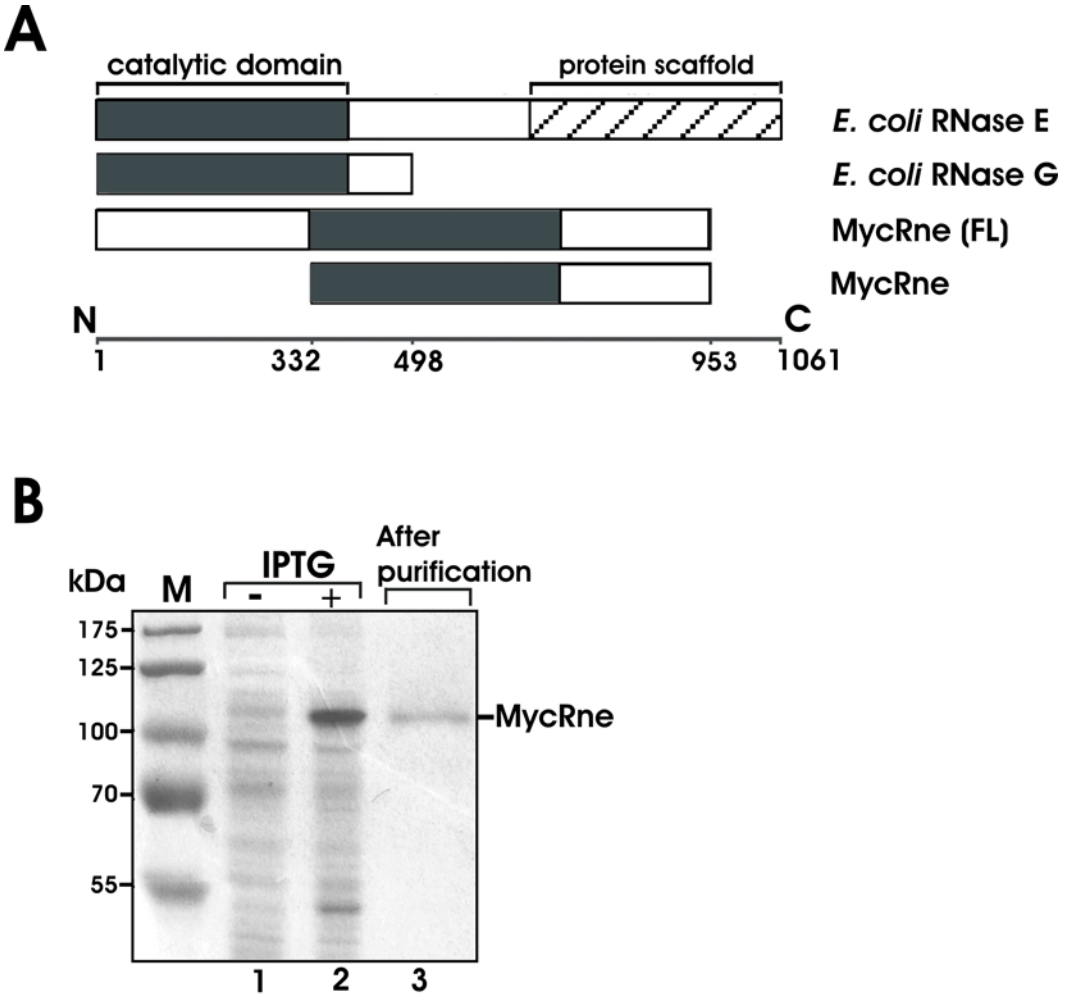

FIG. 1.

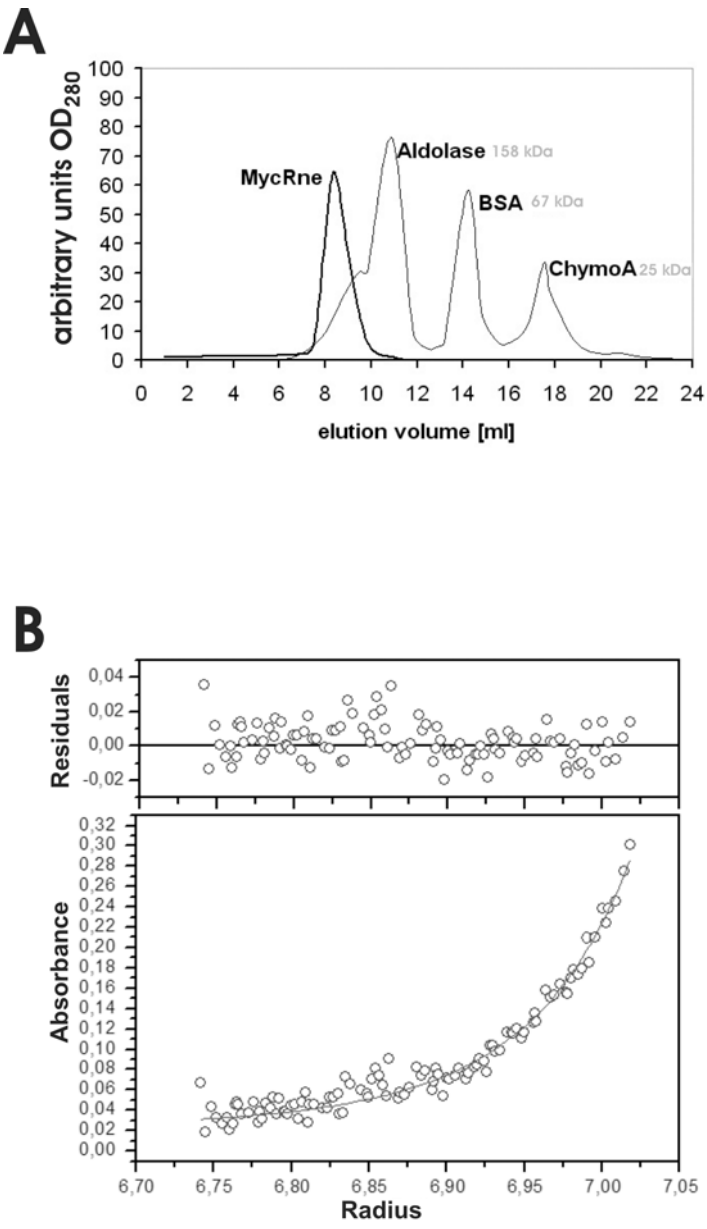

FIG. 2.

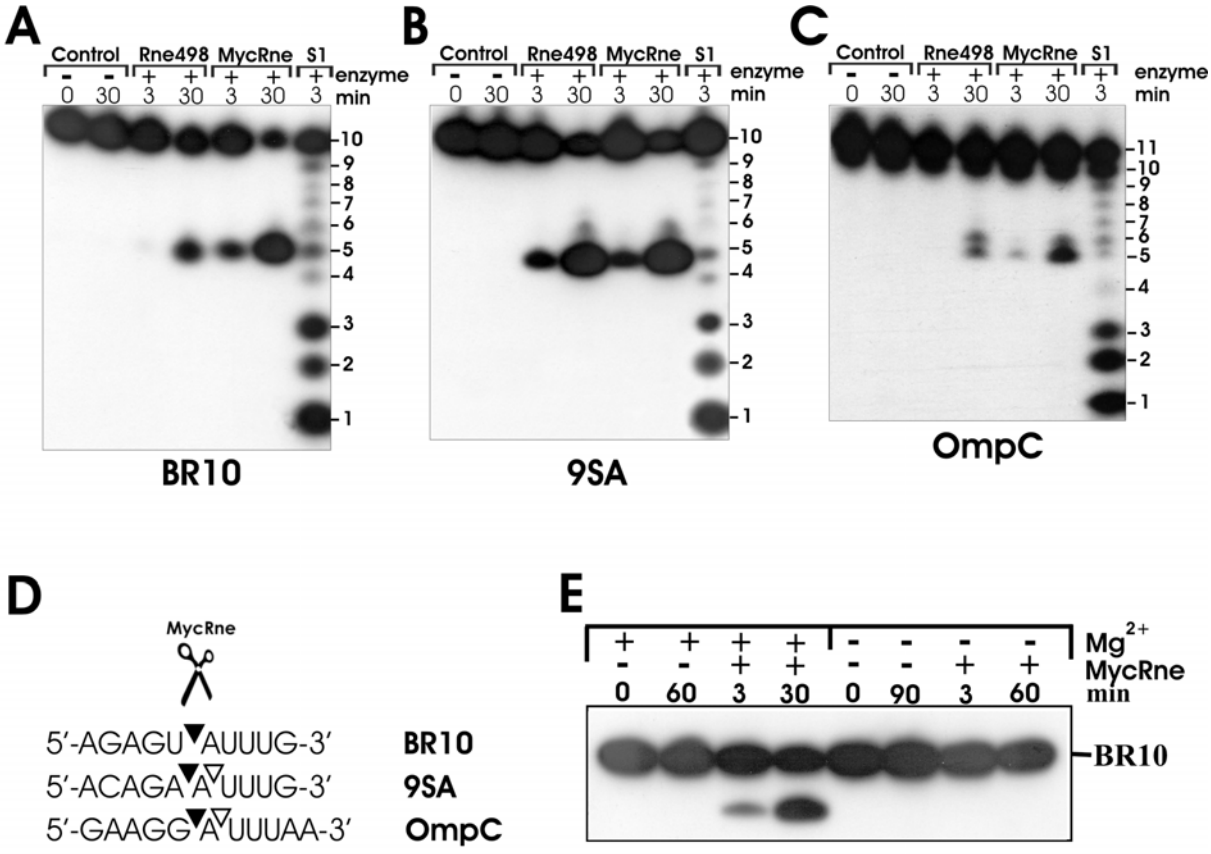

FIG. 3.

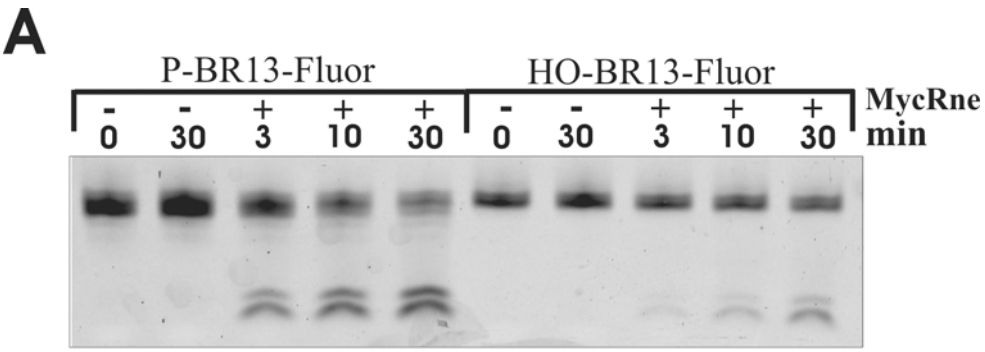

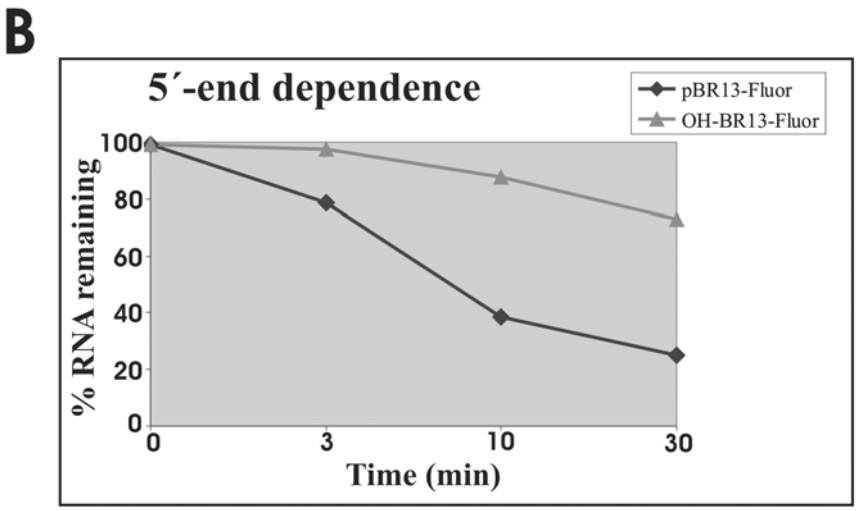

FIG. 4

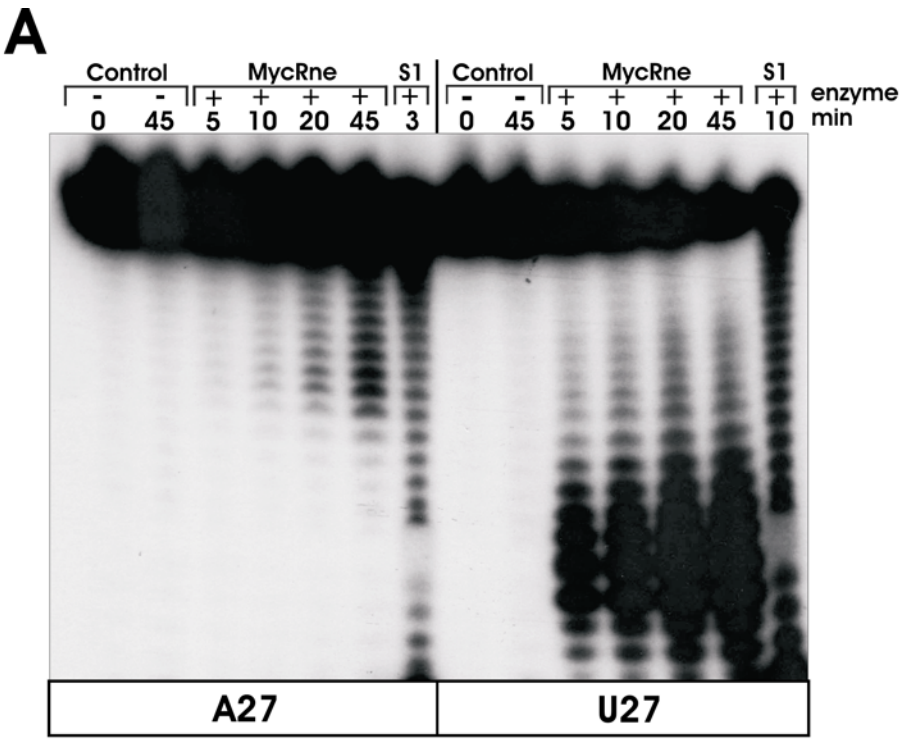

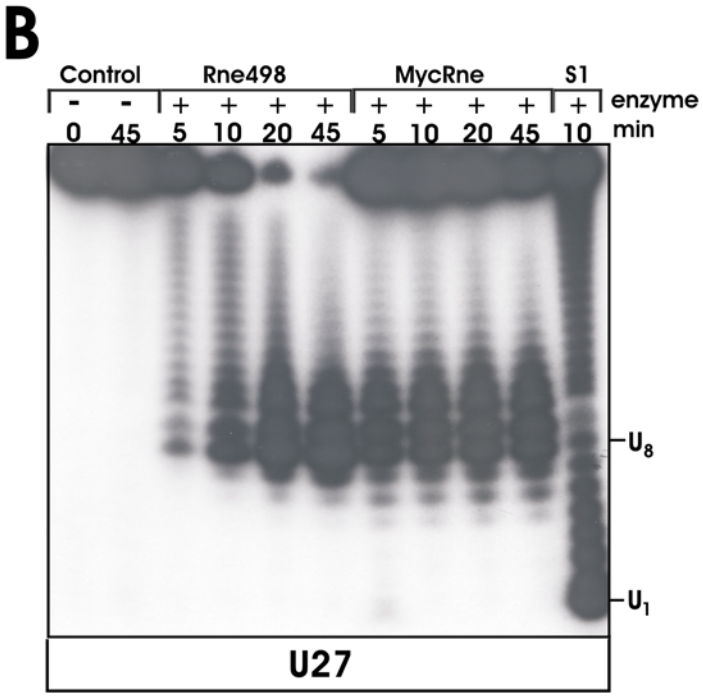

5'-$U_1U_2U_3U_4U_5U_6U_7U_8U_9U_{10}U_{11}U_{12}U_{13}U_{14}...U_{27}$-3' U27 / MycRne

FIG. 5

Biochemical Journal Immediate Publication. Published on 4 Jan 2007 as manuscript BJ20061530

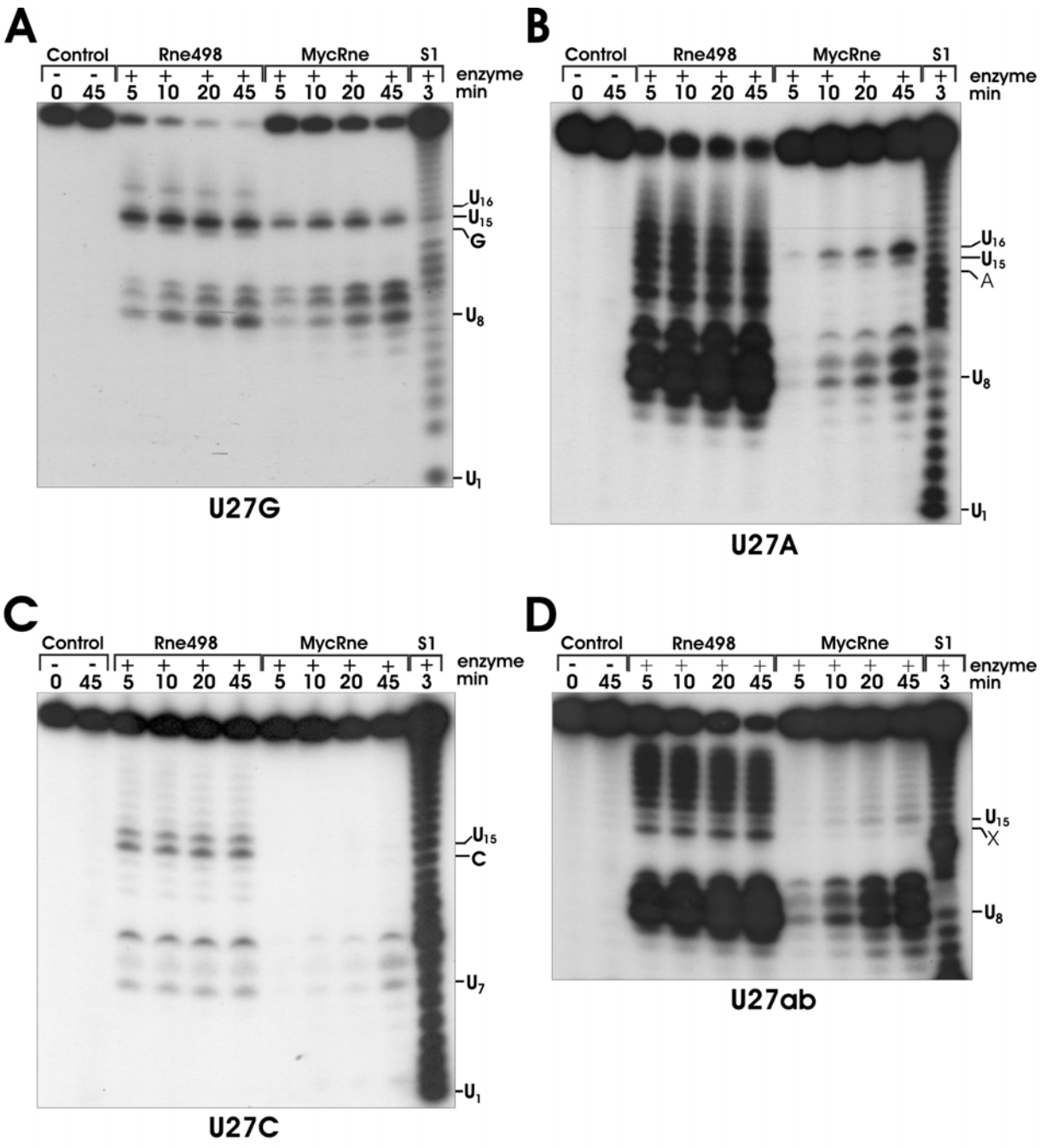

E

5′- $U_1U_2U_3U_4U_5U_6^{\nabla}U_7^{\nabla}U_8^{\blacktriangledown}U_9^{\blacktriangledown}U_{10}^{\blacktriangledown}U_{11}U_{12}U_{13}$ **A** $U_{15}^{\nabla}U_{16}^{\blacktriangledown}U_{17\text{-}27}$ -3′

5′- $U_1U_2U_3U_4U_5U_6^{\nabla}U_7^{\nabla}U_8^{\blacktriangledown}U_9^{\blacktriangledown}U_{10}^{\blacktriangledown}U_{11}U_{12}U_{13}$ **G** $U_{15}^{\blacktriangledown}U_{16}^{\nabla}U_{17\text{-}27}$ -3′

5′- $U_1U_2U_3U_4U_5U_6^{\nabla}U_7^{\blacktriangledown}U_8^{\blacktriangledown}U_9^{\blacktriangledown}U_{10}U_{11}U_{12}U_{13}$ **C** $^{\nabla}U_{15}^{\nabla}U_{16}U_{17\text{-}27}$ -3′

5′- $U_1U_2U_3U_4U_5U_6^{\nabla}U_7^{\nabla}U_8^{\blacktriangledown}U_9^{\blacktriangledown}U_{10}^{\blacktriangledown}U_{11}U_{12}U_{13}$ **X** $U_{15}^{\nabla}U_{16}^{\blacktriangledown}$ (XXXX) -3′

FIG. 6

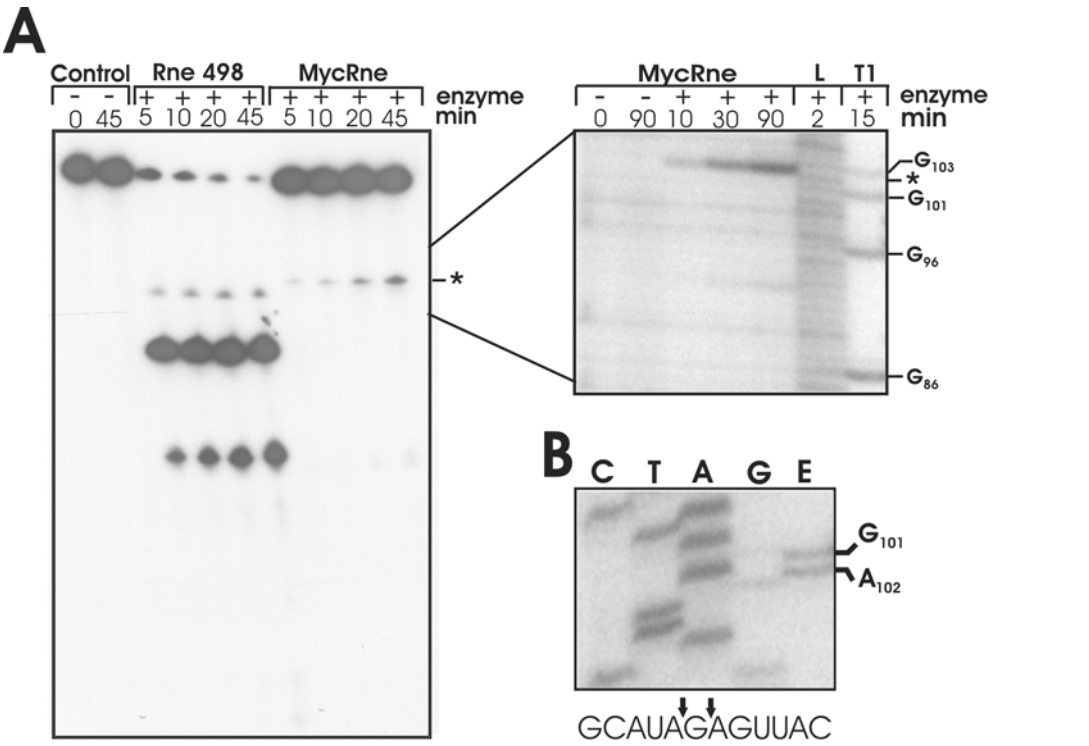

C

5′-CCCUCCCUUUUGGAAAAGGGAGGCAAAAACAAACUCGCAACCACAUCCGUUCACGGCGCU

AGCCGUGCGUCCACACCCCCCACCAGAACAAAUUUGCAUAGAGUUACGGCGGCCACAGCG

GCAGGGAAACGCCCGGUCCCAUUCCGAACCCGGAAGCUAAGCCUGCCAGCGCCGAUGAUA

CUGCCCCUCCGGGUGGAAAAGUAGGACACCGCCGAACA-3′

FIG. 7